Pure Appl. Chem., Vol. 73, No. 6, pp. 897–912, 2001.

INTERNATIONAL UNION OF PURE AND APPLIED CHEMISTRY

MACROMOLECULAR DIVISION
COMMISSION ON POLYMER CHARACTERIZATION AND PROPERTIES
WORKING PARTY ON STRUCTURE AND PROPERTIES OF
COMMERCIAL POLYMERS*

BLENDS CONTAINING CORE-SHELL IMPACT MODIFIERS PART 1. STRUCTURE AND TENSILE DEFORMATION MECHANISMS

(IUPAC Technical Report)

Prepared for publication by
C. B. BUCKNALL
Advanced Materials Department, Cranfield University, Bedford MK43 0AL, UK

Blends containing core-shell impact modifiers
Part 1. Structure and tensile deformation mechanisms

(IUPAC Technical Report)

Abstract: Two impact modifiers, based respectively on polybutadiene (PB) and poly(butyl acrylate-*co*-styrene) (PBA), are compared in blends with four glassy polymers: polycarbonate (PC), poly(methyl methacrylate) (PMMA), poly(styrene-*co*-acrylonitrile) (PSAN), and poly(vinyl chloride) (PVC). Dynamic mechanical tests show glass transitions at about −80 °C in PB and −15 °C in PBA. Both modifiers have grafted PMMA shells, which are seen in the transmission electron microscope (TEM) to be about 10 nm thick. The two-stage PB particles have 200-nm-diameter polybutadiene cores, whereas the three-stage PBA particles have 260-nm-diameter PMMA cores, with 20-nm thick PBA rubber inner shells. Under tension, the PB particles cavitate to form single voids on reaching a critical volume strain, and subsequently offer little resistance to dilatation. By contrast, tensile tests performed *in situ* in the TEM show that the PBA shells form fibrils that are anchored to the rigid core, and act as constraints on further dilatation: the stresses developed in the PBA fibrils can be sufficient to draw fibrils from both the PMMA core and the PSAN matrix. There is evidence that the PMMA shells can debond from the matrix both in cryogenic fracture and in fatigue at 23 °C. Tensile dilatometry shows that the PB particles cavitate at higher strains than the PBA particles, but that the PB particles then cause a rapid volume increase, leading to a low strain at break. By contrast, the PBA particles produce a more controlled dilatation, and higher strains to break. Later papers in this series treat the mechanical and rheological behavior of these blends in more detail.

1. INTRODUCTION

This paper is the first in a series of reports on a collaborative research program undertaken by IUPAC Working Party 4.2.1. The aim of the program is to understand the effects of both matrix and impact-modifier compositions on the properties of rubber-toughened plastics. Four matrix polymers were selected for the program: polycarbonate (PC); poly(methyl methacrylate) (PMMA); poly(styrene-*co*-acrylonitrile) (PSAN); and poly(vinyl chloride) (PVC). Two core-shell impact modifiers were chosen, one based on PB (polybutadiene) and one on PBA [poly(butyl acrylate-*co*-styrene)]. The modifiers were already known to have comparable particle sizes. Blending ratios were calculated with the aim of making materials with equal volume fractions of rubber particles, where the word "particle" includes both the rubber phase itself and any rigid-polymer subinclusions, but excludes the outer shell, which in discussions on mechanical properties is treated as part of the matrix. Both modifiers have grafted PMMA shells.

The active participants in the program are identified by a two-letter code as follows:

BA	BASF AG, Ludwigshafen, Germany	V. Altstädt, H. M. Laun
BP	BP Chemicals, Grangemouth, UK	A. Gray
CR	Cranfield University, Bedford, UK	C. B. Bucknall

EN	Enichem Polymères, Mazingarbe, France	D. Constantin
HU	Hüls AG, Marl, Germany	S. Röber
IC	ICI Technology, Middlesbrough, UK	D. R. Moore
MB	Mobil Chemical, Edison, NJ, USA	B. Gunesin
MF	Montefluos/Ausimont spa, Bollate, Italy	G. Ajroldi
ML	Martin Luther University, Merseburg, Germany	G. H. Michler
NR	National Research Council, Boucherville, Canada	T. Vu-Khanh
SH	Shell, Louvain-la-Neuve, Belgium	L. Glas
SV	Solvay, Brussels, Belgium	C. Dehennau
TD	Technical University of Denmark, Lyngby, Denmark	J. Lyngäae-Jörgensen
TF	Institute of Plastics & Paint Industry, Gliwice, Poland	P. Szewczyk
WA	University of Washington, Seattle, WA, USA	J. C. Seferis
WR	Technical University, Wroclaw, Poland	M. Kozlowski

This paper presents data on the morphology of the blends, as observed by electron microscopy, and on the glass-transition temperatures of the constituent phases. The structures of the modifier particles and the glass transitions of the rubber phases were known to be very different, and were expected to produce differences in deformation and fracture behavior between the two series of blends.

The present paper also examines the effects of structure and morphology upon the micromechanics of tensile deformation in these blends, using both macroscopic specimens and thin sections strained on the electron microscope stage. In the case of PSAN/PBA blends, the *in situ* transmission electron microscopy (TEM) study provided enough detailed information to form a separate paper (Paper 1a), which has been published in another journal [1].

Subsequent reports on this research program will follow a pattern of publication similar to that described above. The overall findings will be published in *Pure and Applied Chemistry*, and more detailed papers on specific aspects of the program will then be prepared for publication in other journals. Papers currently planned for publication are:

Part 2: Melt rheology of rubber-toughened plastics
Part 3: Temperature-induced transitions in tensile impact behavior
Part 4: Temperature-induced transitions in the fracture behavior of unnotched specimens
Part 5: Temperature-induced transitions in the fracture behavior of notched specimens
Part 6: Factors affecting fatigue crack growth behavior

2. MATERIALS

Commercial materials for the program were kindly donated by three companies: Ausimont, ICI, and Rohm & Haas. They are characterized by their manufacturers as:

PC	a general-purpose injection molding grade
PMMA	a medium-molecular-weight injection molding grade
PSAN	a medium-molecular-weight injection molding grade
PVC	a medium-molecular-weight tin-stabilized dry blend, with $K = 53.5$
PB	a polybutadiene-based modifier with a grafted PMMA shell
PBA	a modifier based on poly(butyl acrylate-*co*-styrene) (PBA) elastomer in which the elastomer forms an inner shell, which is grafted to both the PMMA core and the PMMA outer shell

Blends were made in a compounding extruder with co-rotating twin screws at temperatures of:

PC	300 °C	PSAN	280 °C (PB) and 260 °C (PBA)
PMMA	280 °C	PVC	175 °C

Each blend was designed to have a volume fraction of 20% rubber particles. Calculations of the amounts to be blended were based on particles occupying 70% by volume of the diene-based modifier and 60% by volume of the acrylic modifier, the remaining material being in the PMMA shell. The PMMA/PBA blend was transparent at room temperature. The other blends were an opaque white in color.

3. RESULTS

3.1 Transmission electron microscopy

3.1.1 Morphology

Transmission electron microscopy studies aimed at defining particle morphology and spatial dispersion were carried out by Laboratory MB. Pellets of each blend were embedded in epoxy resin, which was then cured at 60 °C before the blend sample was stained with OsO_4 (2% aqueous solution for 2 h at 60 °C) and sectioned at room temperature using a diamond knife. In addition, samples of the neat PBA and PB modifiers were molded, embedded in a support medium, and then sectioned at −90 °C.

As illustrated in Fig. 1, OsO_4 staining of the polybutadiene phase gave excellent contrast with the various matrix polymers. The polybutadiene particles appear to be monodisperse, with diameters of 200 ± 10 nm. The contrast obtained using OsO_4 was not as good in the case of blends based on the PBA modifier. Nevertheless, it was possible to see the particles clearly, and to measure diameters. Unlike the osmium-hardened PB particles, the PBA particles distorted to an elliptical shape, owing to compression by the diamond knife. To allow for this, diameters were determined from the major axes of the ellipses, which are normal to the cutting direction.

Most of the PBA particles had diameters of 300 nm, but a few particles were as large as 500 nm. Each of the 300-nm particles showed an unstained (or understained) core, which is known to consist mainly of PMMA, and a thin stained shell about 20 nm thick, which can be identified as the poly(butyl acrylate-*co*-styrene) elastomer phase. The larger PBA particles had a more complex morphology, with four visible concentric regions: an unstained core and three shells, which were (in order of increasing diameter) stained, unstained, and stained. In blend samples, the outer PMMA shell merges with the matrix polymer, and is therefore not visible in the TEM pictures. However, when molded, the neat PB

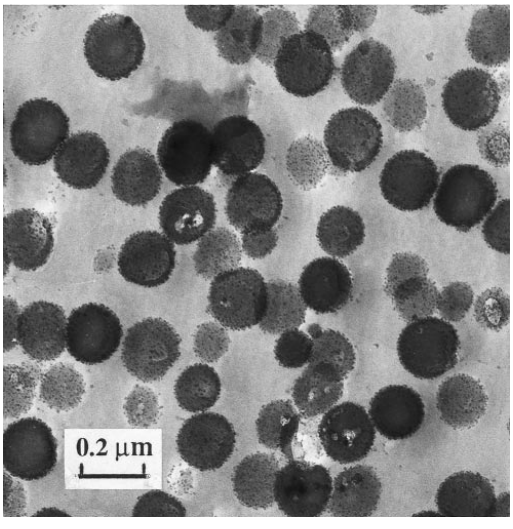

Fig. 1 Osmium-stained section from PSAN/PB blend. Laboratory MB.

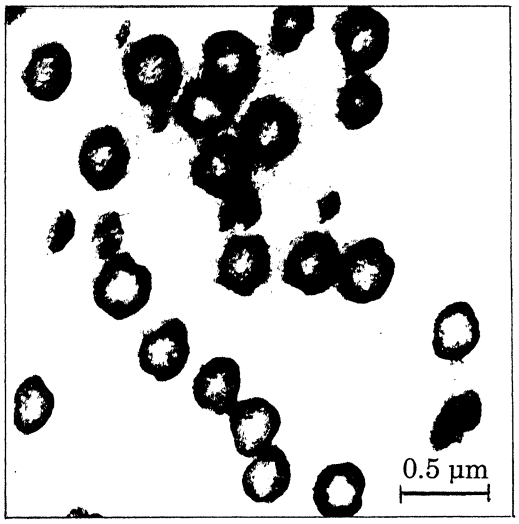

Fig. 2 Ruthenium-stained section from PSAN/PBA blend. Laboratory ML.

modifier showed an unstained honeycomb-like network of PMMA separating the osmium-stained polybutadiene particles. The wall thickness in the honeycomb was 15–20 nm, suggesting a thickness of 8–10 nm for the outer PMMA shells of the original modifier particles.

In a later study, Laboratory ML treated PSAN/PBA blends with RuO_4 to stain the elastomeric poly(butyl acrylate) phase. This procedure provided excellent contrast, as illustrated in Fig. 2, and confirmed that the elastomeric shell was 20 nm thick.

3.1.2 Deformation mechanisms

Laboratory CR carried out a TEM study on ultrathin sections from bars that had previously been subjected to tensile dilatometry tests by Laboratory HU. Blocks from each bar were exposed at room temperature to OsO_4 vapor for 3 days, before being microtomed at room temperature using a diamond knife. No PVC blend samples were available for examination. Certain regions of the PSAN/PB blend showed extensive cavitation of the rubber particles, which occurred mainly in short, connected, angled bands, as shown in Fig. 3. Within the cavitated particles, stretched membranes of rubber spanned the gaps. Some short crazes were also formed in the PSAN matrix.

A small amount of cavitation was also observed in the PC/PB blend, but very few rubber particles were affected, and there was no evidence of crazing. As in PSAN/PB, cavitation was followed by stretching of the rubber phase to very high strains. By contrast, PMMA/PB blends showed only incipient particle cavitation, through the formation of small spherical voids and a limited amount of crazing near the fracture surface. None of the rubber particles in the PMMA blends were highly stretched. The TEM study showed no evidence in any of the PBA blends for either cavitation or craze formation under uniaxial tension. In all six PSAN, PMMA, and PC blends, particle-matrix adhesion appeared to be good, with no sign of debonding even during microtoming. No work was carried out on PVC blends.

Laboratory ML carried out *in situ* TEM studies on thin sections subjected to tensile drawing on the microscope stage. Samples were taken from the middle of compression-molded specimens and microtomed at −110 °C. Sections approximately 1 mm thick were examined at room temperature using a 1000 kV high-voltage electron microscope (HVEM) and sections approximately 0.3 µm thick were studied at three strain rates (0.01, 0.05, and 0.1% s^{-1}) and three temperatures (–20, 23, and 60 °C) using a 200-kV TEM. Because of the range of behavior that it displayed under different test conditions in the TEM, the PSAN/PBA blend was studied in particular detail. Full results are given in a separate paper

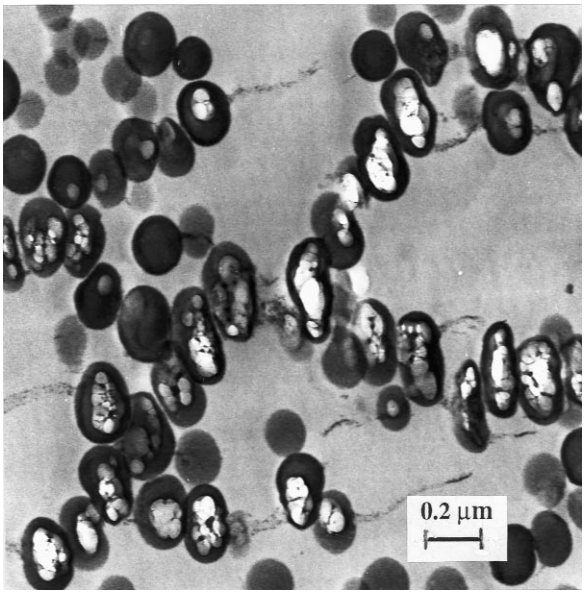

Fig. 3 Osmium-stained section from fractured PSAN/PB tensile bar, showing particle cavitation, dilatation bands, and crazing. Laboratory CR.

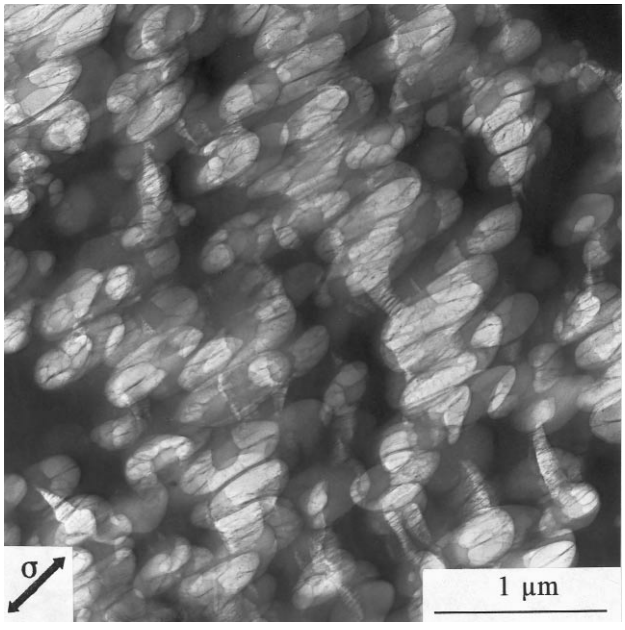

Fig. 4 Section of PSAN/PBA strained *in situ* on the TEM at 23 °C. Arrow shows extension direction. Note fibrillation of shell around PMMA core. Laboratory ML.

[1]. At 23 °C, the grafted PBA shell of the composite rubber particles was observed to cavitate, forming fibrils which radiated from the rigid PMMA core, as shown in Fig. 4. Cavitation provided excellent

contrast in the unstained sections, which show the expanded shell reaching a thickness of ~200 nm. As the original thickness of the PBA shell was only ~20 nm, this figure appears to indicate that the acrylic rubber fibrils have an extension ratio $\lambda = 10$, which is unexpectedly high. A possible explanation is that the fibrillated shell includes some PMMA drawn from the rigid core, and perhaps also from the outer shell, in a process similar to the mechanism responsible for craze thickening.

This view is supported by the HVEM observations illustrated in Fig. 5, which show that the PMMA cores are reduced to thin lenticular remnants. In the transverse direction, these core remnants essentially retain their original dimensions (250 nm); however, in the direction of applied tensile stress they are only 100 nm thick. Clearly, an increasing fraction of the rigid PMMA core is drawn into the surrounding fibrillated shell as the specimen is stretched.

In Fig. 5, about 60% of the PMMA core material appears to have been converted to fibrils. The stresses acting on the fibrillated rubber shell must therefore be very high, because the nominal stresses necessary to maintain fibrillar drawing from a craze wall in PMMA at room temperature are in the range 30–50 MPa, depending upon strain rate. True stresses within the fibrils are, of course, higher than nominal stresses by a factor equal to the draw ratio λ. If PBA constitutes 50% of the fibrillated polymer shell, λ has a value of about 5. At 23 °C, cavitation of the PBA particles in PSAN blends is accompanied by shear yielding, plus a limited amount of crazing, in the matrix. At −20 °C, the modifier particles cavitate through fibrillation of the PBA shells, as at room temperature, but the dominant deformation mechanism in the PSAN matrix changes to multiple crazing, with no evidence of shear yielding. By contrast, when the test temperature is raised to 60 °C the modifier particles cavitate in a manner similar to that of PB particles at room temperature, leaving no sign of the original PMMA core or of the elastomer shell, with only thin membranes of polymer stretched across the cavity. These observations suggest that the reduced resistance of PMMA to drawing at elevated temperature results in complete disruption of the rigid core during *in situ* tensile tests in the TEM. At 60 °C, shear yielding is the predominant deformation mechanism in the PSAN matrix, and there is no evidence of crazing.

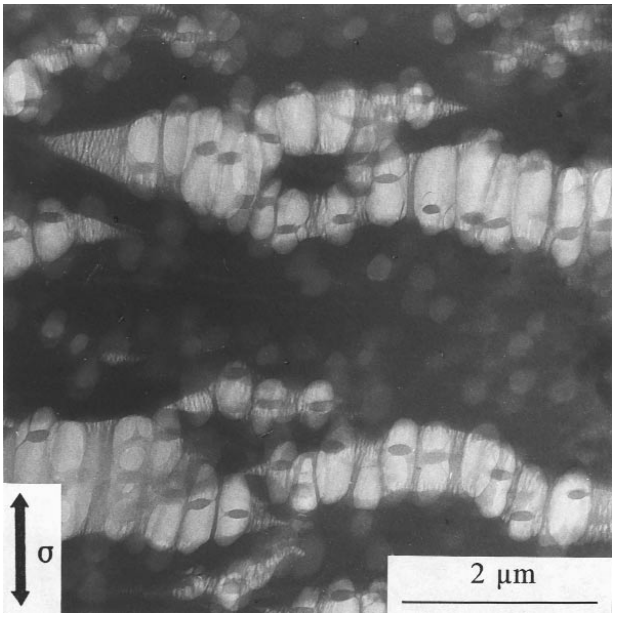

Fig. 5 Section of PSAN/PBA drawn to high strain in HVEM. Arrow shows draw direction. Note flattened remnants of disrupted PMMA core. Laboratory ML.

3.2 Scanning electron microscopy

Scanning electron microscopy (SEM) was carried out by Laboratory EN on specimens cut from a compression-molded sheet with a thickness of 0.2 mm, which were fractured at liquid nitrogen temperatures. Fracture surfaces were coated with gold before SEM examination. In another experiment, blends containing polybutadiene were microtomed at room temperature using a diamond knife to prepare a flat surface, which was then stained with OsO_4 (24 h in 1% aqueous solution) before being coated with carbon in a vacuum evaporator. Blends of the PB modifier with PSAN and PMMA showed some evidence in places of poor dispersion on a macroscopic scale, which was evident to the naked eye. The other blends appeared to have a satisfactory degree of dispersion.

Blends of PC with both modifiers show considerable ductility on the fracture surfaces, despite the extremely low fracture temperatures. Both PVC blends also provide evidence of extensive low-temperature ductility, but to a lesser extent than in the case of PC blends; some debonded spheres can be seen on the fracture surface. Blends based on PMMA and on PSAN appear to be much more susceptible to particle-matrix debonding during cryogenic fracture; at high magnification, fracture surfaces of PMMA/PB blends are marked with distinct spherical projections and cavities, both about 200 nm in diameter. Fewer and smaller spheres can be seen on the surface of PMMA/PBA blends, and there is little sign of cavitation. Similar features are seen in PSAN/PBA blends. The PSAN/PB blend shows two types of fracture surface, one dominated by 200-nm spherical projections, and the other featuring hollows of similar size.

Laboratory BA examined the fracture surfaces of fatigue specimens at three points along the path of the crack. The specimens were tested at 23 °C and 1 Hz, and coated with gold before examination. At high magnifications, the PVC blends show ductile deformation, with some cavitation. In PVC/PBA blends, fracture surfaces also show evidence of retracted broken fibrils (seen as projecting nodules about 50 nm across) and small spherical particles attached by fibrils to the matrix. These latter features might be retracted craze fibrils, debonded modifier particles, or residual cores left behind after fibrillation and failure of the acrylic rubber shell. Some spheres of similar size to the rubber particles can be seen in PVC/PB blends, but are relatively infrequent. In both PC blends, ductile drawing is the main deformation mechanism. Cavitation is prominent in PC/PB blends, but less obvious in PC/PBA blends. Blends of PB and of PBA with both PMMA and PSAN show signs of cavitation and fracture of fibrils. Fine 50-nm nodules, which are probably formed through fracture of craze fibrils, are most pronounced in PSAN/PB blends, although they are present on the fracture surfaces of all four PMMA and PSAN blends, together with more rounded nodules of similar size to the modifier particles.

Laboratory BA also made a more detailed SEM study of PSAN/PB fatigue specimens, to determine whether cavitation of the rubber particles or debonding from the PSAN matrix was responsible for the depressions seen on fracture surfaces. These surfaces were stained with OsO_4 before being sputter-coated with a thin carbon layer to provide conductivity. Specimens were examined using the dual electron detector system illustrated in Fig. 6. One detector collected the slow secondary electrons, which provide information about the topology of the surface, while another collected the fast primary electrons back-scattered from material lying close to the surface. At any given energy of the incident electrons, the probability of back-scatter is approximately proportional to the atomic number of the target atoms. The presence of osmium-stained rubber particles at or immediately below the fracture surface is therefore easily detected. As illustrated in Fig. 7, the particle sizes observed using back-scattered electrons are consistently smaller than the hemispherical projections observed in the corresponding secondary electron image. Clearly, the surfaces of the hemispherical projections are covered with an unstained layer of glassy polymer, which is almost certainly composed largely of grafted PMMA. This result confirms the observation of Laboratory EN, that PMMA-coated modifier particles tend to debond from the PSAN matrix under critical loading conditions.

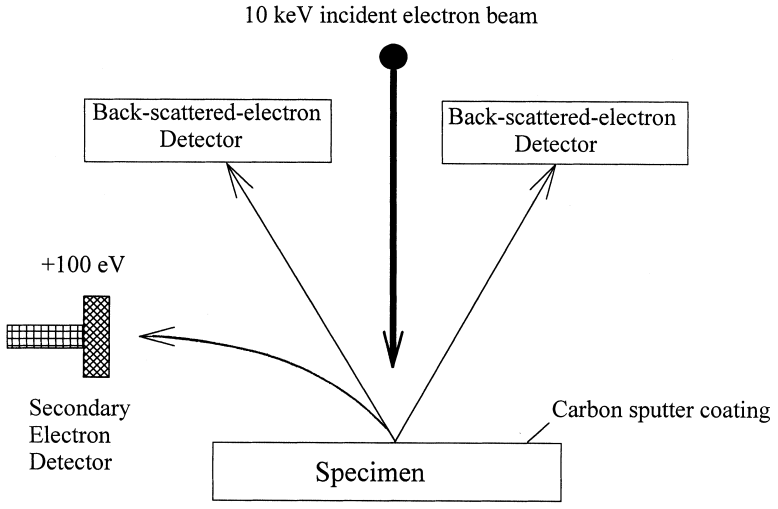

Fig. 6 Positions of secondary-electron and back-scattered-electron detectors in SEM. Laboratory BA.

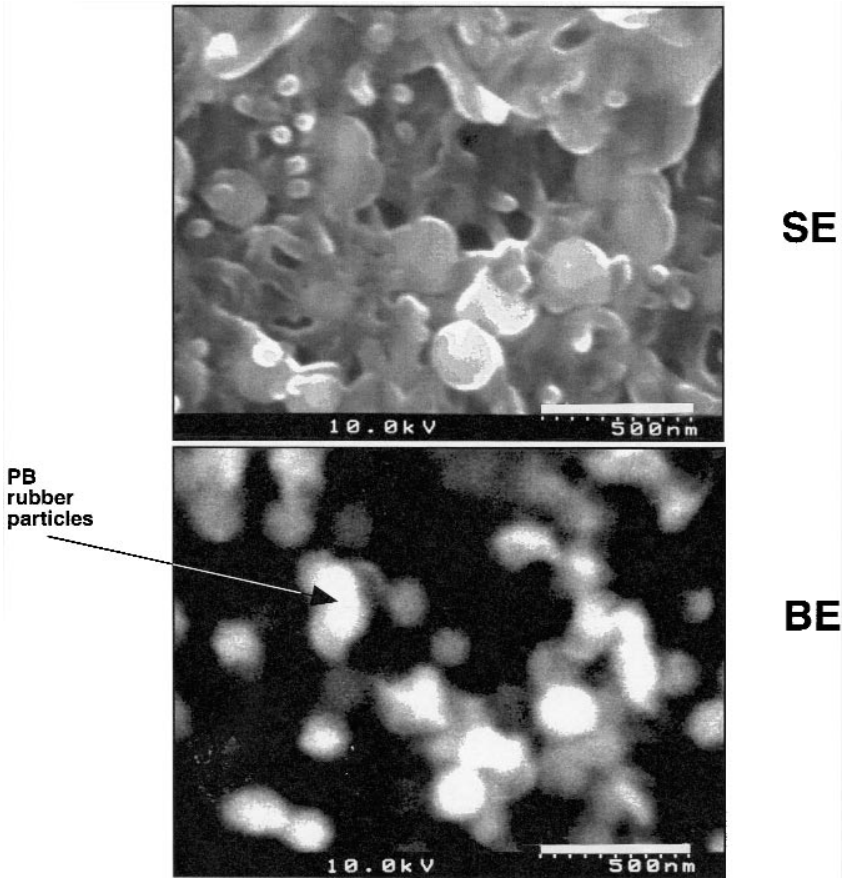

Fig. 7 SEM image of a fatigue fracture surface of a PSAN/PB blend observed using secondary-electron (SE) and back-scattered-electron (BE) detectors. Laboratory BA. Scale bar 500 nm.

3.3 Relaxation temperatures

Three laboratories (MF, NR, and WA) made measurements on the relaxation temperatures of elastomer and matrix components of the blends. Their data are summarized in Tables 1 and 2 and Fig. 8. They provide a comparison between different methods for determining transitions, as defined by peaks in dynamic mechanical curves, and by changes in thermal expansion behavior. Laboratory MF used a Brabender Torsion-automat torsion pendulum, following ISO method R 537-B. Laboratory NR made measurements using a Polymer Laboratories Mk II DMTA machine at a frequency of 1 Hz. Laboratory WA made measurements using a DuPont 983 DMA at a heating rate of 5 °C/min. Specimens were not predried.

Measured values of T_g for the elastomer phase vary quite widely with both test method and type of matrix. It can be seen that PB blends undergo a transition at about −75 °C, corresponding to the T_g of the chosen polybutadiene, and that the PBA shows a transition at about −10 °C, which is significantly higher than the expected T_g of the poly(butyl acrylate-*co*-styrene). These results suggest that sequential emulsion polymerization produces an upward shift in the glass transition of the rubber phase, especially in the case of PBA. There is also a considerable variation in the measured T_g values for the matrix polymers, which suggests that heating rates, test frequencies, and other factors affect the results.

In addition to the major relaxations due to the glass transitions of elastomer and matrix polymer, several secondary transitions are seen in the dynamical mechanical spectra. Laboratory MF observed β-transitions in PC at −90 °C, in PVC at −60 °C, and in PMMA at about +30 °C, the latter peak forming a very broad shoulder running up to the α transition in PMMA. Laboratory NR found a prominent sec-

Table 1 Transition temperatures (°C) in elastomers with differing matrices and test procedures. ND = No Data. Here E'' is the imaginary component of modulus, J'' is the imaginary component of compliance, and δ is the phase angle.

Elastomer	Laboratory	Method	PC	PMMA	PSAN	PVC
PB	WA	log J"	–69	–78	–73	ND
	WA	log E"	–71	–82	–74	ND
	WA	log tan δ	–71	–78	–74	ND
	NR	E"	–73	–76	ND	ND
	MF	log tan δ	–80	–85	–86	–86
PBA	WA	log J"	+4	+1	+2	ND
	WA	log E"	–5	–4	–1	ND
	WA	log tan δ	0	+1	–5	ND
	NR	E"	–17	–16	ND	ND
	MF	log tan δ	–15	–15	–17	–18

Table 2 Transition temperatures (°C) in matrix polymers with differing elastomers and test procedures. Laboratories as listed in Table 1. In the log tan δ column, two sets of data are given, from Laboratories WA (left) and MF (right) respectively. ND = No Data.

Matrix	Elastomer	Expansion	log J"	log E"	log tan δ		E"
PC	PB	151	ND	153	159	144	144
	PBA	150–153	ND	153	159	145	145
PMMA	PB	115–120	148	117	135	117	110
alpha	PBA	112–120	ND	117	136	117	109
PMMA	PB	ND	ND	10	19	60	15
beta	PBA	ND	ND	ND	ND	60	ND
PSAN	PB	106–110	ND	114	122	117	ND
	PBA	112	ND	117	125	104	ND

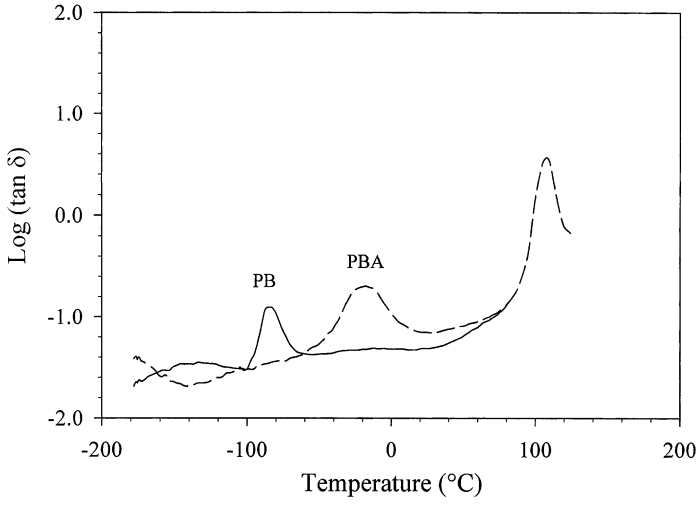

Fig. 8 Dynamic mechanical loss curves for PSAN/PB and PSAN/PBA blends. Laboratory MF.

ondary relaxation in PMMA at 15 °C, which can clearly be identified with the peak at +30 °C noted by Laboratory MF.

3.4 Tensile yield and fracture

Tensile tests were carried out at 23 °C and −10 °C by Laboratory TF, at crosshead speeds of 1 and 50 mm/min, using 3-mm-thick specimens with dimensions according to ISO/DIN 527-2. Table 3 summarizes the results in terms of yield stress σ_y, extension to break ε_f, and stress at break σ_f. Each figure is

Table 3 Tensile test data at 23° and –10 °C (Laboratory TF). ND = No Data.

			PSAN		PMMA		PVC		PC	
	Speed mm min^{-1}	Unit MPa %	PB	PBA	PB	PBA	PB	PBA	PB	PBA
23 °C		σ_y	40.7	41.7	42.3	38.1	30.4	32.5	33.6	32.6
	1	ε_f %	10.1	63.0	45.5	47.7	101.7	104.2	110.8	115
		σ_f	36.1	34.7	33.9	35.9	26.0	34.2	41.9	47.7
		σ_y	47.4	48.9	54.3	47.4	37.8	38.6	38.7	36.6
	50	ε_f %	13.0	25.0	19.0	27.8	26.2	69.2	115.8	102
		σ_f	38.5	38.4	42.3	42.0	26.0	31.2	42.4	45.5
–10 °C		σ_y	NY	57.0	63.9	56.8	ND	ND	43.9	43.6
	1	ε_f %	7.9	26.7	12.5	19.2			100.0	84.2
		σ_f	58.8	52.9	58.9	54.3			51.4	54.8
		σ_y	NY	65.6	NY	68.0	ND	ND	49.2	50.2
	50	ε_f %	7.5	13.3	7.9	10.4			108.3	56.3
		σ_f	55.8	58.3	71.8	71.3			52.7	51.2

the mean of 3–5 readings. For the PVC/PB blend tested at 50 mm/min, 2 out of 4 specimens failed at a very low strain (ε_f = 1.0 to 1.3%). Tests at 23 °C show that the PC blends are capable of reaching deformations ε_f in excess of 100%, and exhibit a marked degree of strain hardening, as indicated by a ratio $\sigma_f/\sigma_y > 1$. There is some reduction at −10 °C in the ε_f of PC/PBA blends, especially at the higher strain rate, but both PC/PBA and PC/PB blends show a high level of ductility. Blends based on PVC, PMMA, and PSAN show a much more marked dependence of ε_f upon strain rate, temperature, and type of impact modifier. None of the other matrices provides the same degree of strain hardening as PC, and only PC and PVC blends reach extensions greater than 80%. Only in PC at 10 °C does the PB modifier give significantly higher ε_f than the PBA modifier, which is close to its T_g at this temperature. In a few cases the two modifiers are equal in their performance, but in the majority of cases, higher elongations are reached in blends containing PBA. This difference may be due to the stabilizing influence of a load-bearing fibrillated rubber phase bonded to a rigid central core, as shown in Fig. 4. Stabilization of this kind might not be important in PC, where the matrix deforms predominantly by shear yielding, and exhibits strong strain hardening effects. However, the stabilizing effect of fibrillated rubber is probably critical in matrices that are more susceptible to crazing, since void formation is often the first stage of craze failure.

3.5 Tensile dilatometry

Volumetric changes were measured by Laboratory HU during tensile tests on PC, PSAN, and PVC blends, using a water immersion dilatometer. Data are shown in Fig. 9. They show significant differ-

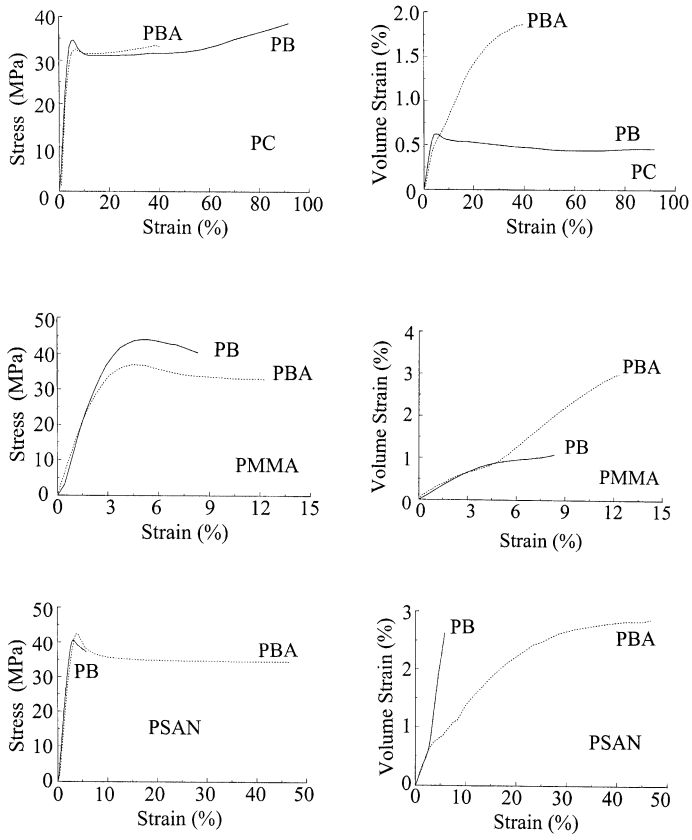

Fig. 9 Stress-strain curves and corresponding tensile dilatometry curves of volume strain against (tensile) strain. Laboratory HU.

ences between the matrix polymers and between the two modifiers. Postyield deformation in blends of PBA with PC and with PSAN produces a volume increase of about 2%, as the specimen extends plastically by 40%. In the case of the PMMA/PBA blends, cavitation occurs more rapidly, with a 2% increase in volume strain developing during an extension of only 7%.

Blends containing PB behave quite differently. Those based on PC and PMMA show little or no increase in volume after reaching the yield stress, whereas the blend of PB with PSAN develops a rapid increase in volume after reaching the yield stress, followed by an early break at about 6% extension. For the PSAN/PB blend, the slope $dV/d\varepsilon$ is 0.7 after yielding. In both PC and PMMA, blends containing PB necked after yielding, and deformation was clearly dominated by shear yielding occurring essentially at constant volume.

4. DISCUSSION

This work has shown that the mechanisms of deformation operating in rubber-toughened blends depend upon the properties of the matrix polymer, the characteristics of the impact modifier, and the test conditions. The choice of matrix polymer is perhaps the most important of these factors. All four of the glassy polymers chosen for this study are capable of deforming by shear mechanisms at room temperature, and therefore of producing a ductile response to tensile loading, but the degree of ductility that they display depends upon their resistance to crazing, which decreases in the order PC, PVC, PMMA, and PSAN. This order is determined by entanglement density [2,3] and by the shear yield stress of the glassy polymer. The ductility of polycarbonate is a consequence of both its high chain entanglement density and its relatively low yield stress: by comparison, PSAN has a lower entanglement density and a higher shear yield stress; while PMMA has a similar entanglement density to PC, but a higher shear yield stress as determined in compression tests [4].

Reducing the test temperature or increasing the strain rate raises the shear yield stress, thus increasing the extent of crazing at a given stage of deformation. These trends are reflected in electron microscopy observations on impact-modified blends. Crazing occurs most prominently in PSAN/PB blends, especially at low temperatures, and gradually gives way to shear yielding as the temperature is raised to 60 °C. Tensile dilatometry provides quantitative confirmation that some combination of rubber particle cavitation and matrix crazing is the main mechanism of tensile deformation in this blend at 23 °C.

The effects of molecular characteristics upon crazing, shear yielding, and fracture of glassy polymers have been studied over many years. One of the most important advances was the demonstration by Donald and Kramer [2,3] that the natural (maximum) draw ratio λ_{max} of crazes in noncrystalline thermoplastics is related to entanglement density. Values of λ_{max} for PC, PMMA, and PSAN (24% AN) are respectively 2.5, 2.6, and 3.3. These figures rank the three polymers in order of decreasing resistance to craze formation. Perhaps of equal significance is the correlation found by Vincent [5] between tensile strength at the ductile-brittle transition and the cross-sectional area of the polymer molecules. Figures for polystyrene, PMMA, PC, and PVC are respectively 1.35, 1.50, 3.04, and 3.40 bonds per nm^3. Using Vincent's method, the estimated figure for PSAN is 1.63 bonds per nm^3. A combination of a low natural draw ratio and a high concentration of load-bearing main-chain chemical bonds enables a polymer to strain harden and reach large tensile strains before crazing and fracture. These features provide an explanation for the observation that PC and PVC blends have higher strains to break than PMMA and PSAN blends.

The interface between rubber particles and matrix polymer is also critical. Debonding of the modifier particles from the surrounding matrix is observed in PSAN, PMMA, and (to a lesser extent) PVC blends fractured at liquid nitrogen temperatures, and in specimens of the PSAN/PB blend subjected to fatigue tests at 23 °C. However, under other test conditions the adhesion between the various matrix polymers and the PMMA shells of the modifier particles appears to be satisfactory. There is no evidence of debonding in any of the thin sections, even at the very large strains reached in the *in situ* tensile tests

in the TEM. As PMMA is one of the matrix polymers that shows extensive debonding in cryogenic fracture, and as blends based on all of the four matrix polymers reach strains of over 40% in at least one type of tensile test, it must be concluded that the presence of an interface between two dissimilar glassy polymers does not detract significantly from the ability of the core-shell modifier particles to toughen PC, PSAN, or PVC.

The most important results from the present study are those relating to the cavitation of the rubber particles. Firstly, TEM shows that the two particle morphologies result in two distinct types of cavitation. The homogeneous PB particles form a single cavity which expands freely during the subsequent tensile deformation of the matrix, whereas the PBA particles undergo fibrillation of the elastomeric shell, which then develops by drawing PMMA fibrils from the rigid core of the particle, and possibly also from the outer shell and surrounding matrix. The resulting partial disruption of the central core in PBA particles, with the formation of a lens-shaped residue, has not previously been reported, and constitutes a new mechanism of energy absorption in rubber-toughened plastics. The observations on PSAN/PBA blends at 60 °C, where no PMMA cores can be seen after drawing in the TEM, suggests that this process of disruption of the core can continue to completion under certain conditions, notably when the resistance to tensile drawing is lower in PMMA than in the matrix polymer.

Another important conclusion from the observations is that the stresses acting within the rubber particles are relatively high and comparable with those necessary to draw fibrils from the walls of crazes (i.e., in the order of 30 MPa). This means that PBA particles share the applied stress with neighboring matrix material, thereby reducing the probability of fracture.

Tensile dilatometry provides further insight into the cavitation process. The PC/PB blend reaches very large strains, essentially at constant volume: the measured volume strain of 0.5% is due simply to the elastic response of the material to the mean stress. The PC/PBA blend, on the other hand, shows a small but steady increase in volume with increasing tensile strain. It is clear that the PB particles are more resistant than the PBA particles to cavitation. This difference can be attributed to differences in particle size. The energy-balance model developed by Bucknall *et al.* predicts that the critical volume strain required to initiate cavitation in rubber particles increases approximately as the reciprocal of particle diameter, other factors being equal [6,7]. In applying the cavitation model to the PB and PBA particles of the present study, due account must be taken of the rigid core in the PBA particles, and of differences in shear modulus between the two rubbers. However, the larger size of the PBA particles appears to be the main factor controlling cavitation resistance.

Another factor that must be noted is the restraining effect of the fibrillated PBA shell on subsequent dilatation of the matrix. Immediately after the onset of cavitation, when the PBA shell contains only a single small void, the resistance to dilatation is very low. As the remainder of the rubbery shell fibrillates, it expands rapidly to several times its original thickness. Thereafter, the restraining effect of the core, and load-sharing between rubber fibrils and matrix, limit the rate of volume increase with tensile strain.

A similar effect is seen in PSAN/PBA blends, where again the rate of dilatation is relatively low. This contrasts strongly with the rapid dilatation of the PSAN/PB blend, which from TEM studies is known to be due to cavitation of the rubber particles, accompanied by crazing of the matrix. The dilatometry data indicate that the PB rubber particles in PSAN reach the critical volume strain required for cavitation, and that having done so, they exhibit a much lower resistance to subsequent dilatation than that shown by fibrillated PBA particles. The reason for this difference can be found in the stress distributions within the rubber phase. In a cavitated sphere, the stresses are much higher in a small region near the surface of the void, where the rubber membranes have reached their maximum extension and are about to tear further, than they are elsewhere in the particle [6]. In a fibrillated rubber particle, on the other hand, the distribution of stresses acting on the fibrils is much more uniform.

In comparing the mechanical properties of the eight blends prepared for this program, due account must be taken not only of differences in particle morphology, but also of the large difference in

glass transition temperature between the two rubbers. The effects of this difference can be seen to some extent in the tensile data for −10 °C presented in Table 3. Later papers in this series will present the results of fracture tests carried out over a range of temperatures and test conditions, including tensile impact, dart-drop impact on plates, Charpy impact, and fatigue. The emphasis in these papers will be upon the factors affecting the ductile-brittle transition temperature in PB and PBA blends, and the extent to which the information about morphology, tensile deformation mechanisms, and relaxation behavior discussed in this paper can be used to interpret the fracture data.

5. CONCLUSIONS

This paper has demonstrated major differences in deformation behavior between two similar core-shell impact modifiers, in blends with polycarbonate, PMMA, poly(styrene-*co*-acrylonitrile) and PVC. Both modifiers have grafted PMMA outer shells. In one case, the core of the particle is a homogeneous sphere of cross-linked polybutadiene approximately 200 nm in diameter. In the other, the core is a PMMA sphere approximately 260 nm in diameter, which is surrounded by a 20-nm-thick inner shell of poly(butyl acrylate-*co*-styrene). The smaller PB particle is more resistant to cavitation, but once cavitated it offers little resistance to further dilatation. By contrast, the complex PBA-based particle is easier to cavitate, but exerts strong control on subsequent dilatation. The differences in initial cavitation resistance in the rubber particle can be explained by an energy balance model [6–8]. The differences in subsequent dilatation behavior can be related to the way in which cavitation develops. Homogeneous rubber particles essentially undergo internal tearing around a single void, whereas particles containing constrained shells of elastomer form fibrils, which are capable of carrying large stresses.

The study has identified a new mechanism of energy absorption in rubber-toughened plastics, involving fibrillation of the rigid glassy core in the PBA particles as the elastomeric shell to which it is grafted is strained radially by the matrix.

ACRONYMS AND ABBREVIATIONS

PB	polybutadiene: The letters are used to denote both the elastomer itself and the modifier in which the elastomer is the main constituent.
PBA	poly(butadiene-*co*-styrene): The letters are used to denote both the elastomer itself and the modifier in which the elastomer is the main constituent.
PC	polycarbonate (of Bisphenol A)
PMMA	poly(methyl methacrylate)
PSAN	poly(styrene-*co*-acrylonitrile)
PVC	poly(vinyl chloride): the rigid form, without plasticizer
TEM	transmission electron microscope/microscopy

The following two-letter acronyms are used to identify active participants: BA, BP, CR, EN, HU, IC, MB, MF, ML, NR, SH, SV, TD, WA, and WR. See Section 1, Introduction, for details.

REFERENCES

1. J. U. Starke, R. Gotehardt, G. H. Michler, C. B. Bucknall. *J. Mater. Sci.* **32**, 1855 (1996).
2. A. M. Donald and E. J. Kramer. *J. Polym. Sci. (Polym. Phys. Ed.)* **20**, 899 (1982).
3. A. M. Donald and E. J. Kramer. *Polymer* **23**, 461 (1982).
4. J. M. Gloaguen, P. Steer, P. Galliard, C. Wrotecki, J. M. Lefebvre. *Polym. Eng. Sci.* **33**, 748 (1993).
5. P. I. Vincent. *Polymer* **13**, 558 (1972).
6. A. Lazzeri and C. B. Bucknall. *J. Mater. Sci.* **28**, 6799 (1993).

7. C. B. Bucknall, A. Karpodinis, X. C. Zhang. *J. Mater. Sci.* **29**, 3377 (1994).
8. A. Lazzeri and C. B. Bucknall. *Polymer* **36**, 2895 (1995).